PERGAMON

Physics and Chemistry of the Earth xxx (2002) xxx–xxx

PHYSICS and CHEMISTRY of the EARTH

www.elsevier.com/locate/pce

Assimilation of TOPEX/Poseidon data in a global ocean model: differences in 1995–1996

Manfred Wenzel *, Jens Schröter

Alfred Wegener Institute for Polar and Marine Research, P.O. Box 120161, D-27515 Bremerhaven, Germany

Abstract

Starting from an optimized climatological ocean model two response experiments are performed to study the impact of assimilating altimeter data on the ocean state. For this purpose TOPEX/Poseidon altimeter measurements from 1995 and 1996, respectively, are used. The model setup remains the same in the reference and the response experiments except the relative weight of the altimeter data is increased for the new assimilation experiments. Furthermore a cyclic repetition of altimeter data from the respective years will be used instead of a mean annual cycle. The analysis of the differences in the two 'perpetual 1995' and 'perpetual 1996' solutions shows that the changes in the optimal forcing are small and differences in the flow fields are noticeable only in the upper ocean. The model is able to follow the different sea surface height measurements by adjusting the upper ocean thermal and haline structures. The modelled steric height anomalies closely follow the TOPEX/Poseidon anomalies. These anomalies are mainly due to thermal expansion while the haline expansion is a second order effect in most parts of the global ocean. Nevertheless the latter cannot be neglected anywhere because it at least partly compensates the thermal.

Keywords: Sea surface heights; Data assimilation; TOPEX/Poseidon; Steric effect

1. Introduction

According to Gill and Niiler (1973) the variability of the sea surface height (SSH) is to first order due to changes in the ocean heat content (thermal expansion) while the effect of salinity changes plays only a secondary role. However Maes (1998) and Sato et al. (2000) recently demonstrated the importance of the halosteric effect on SSH changes. Similar results are obtained by Levitus and Antonov (2002) who investigate the influence of temperature and salinity changes on the dynamic topography from measurements. A further prominent source of SSH variations is the adjustment of the ocean to varying windstress fields via planetary waves (Stammer, 1997; Vivier et al., 1999).

The variational optimization or adjoint method provides us with a powerful tool to estimate an ocean state that is consistent with both, the given model equations and the data. This is done by optimizing certain parameters that control the models evolution in space and time: the models initial state and the surface forcing fields. Wenzel et al. (2001) (WSO hereafter) used this method to estimate the climatological annual cycle of the ocean. Here we will employ this method to study, how it explains the interannual SSH variations as given by the TOPEX/Poseidon altimeter measurements: by changing the models thermo-haline structure, changing the external forcing or both.

2. Method and data

The purpose of this study is to obtain a global ocean model state that evolves according to the model equations and that matches the SSH as measured by the TOPEX/Poseidon altimeter mission in 1995 and 1996 as close as possible. As in WSO we will employ the Hamburg LSG model (Maier-Reimer and Mikolajewicz, 1991), where LSG stands for 'Large Scale Geostrophic'. This model was originally designed for ocean climate studies, but has been used successfully for many other purposes (e.g. Maier-Reimer et al., 1993). Here we will use the coarse resolution LSG with $3.5° \times 3.5°$ effective horizontal grid spacing and 11 layers in the vertical. The great advantage of this model is the implicit formulation in time, which allows for a timestep of one month.

* Corresponding author. Tel.: +49-471-4831-1763; fax: +49-471-4831-1797.
E-mail address: mwenzel@awi-bremerhaven.de (M. Wenzel).

1474-7065/02/$ - see front matter © 2002 Published by Elsevier Science Ltd.
PII: S1474-7065(02)00086-4

To combine the model and the data we use the adjoint method, that is based on the ideas of Marchuk (1975), LeDimet and Talagrand (1986) and others. A detailed description can be found e.g. in Thacker (1988). The adjoint method is a variational optimization method that adjusts the models trajectory in space and time to the data by optimizing certain control parameters while minimizing a cost function. The cost function describes e.g. the squared distance between the data and the corresponding model values. It may also comprise constraints on the parameters themselves. A more detailed description on the implementation of the method and the employed cost function can be found in WSO. The final experiment therein, denoted FIN, describes the models optimal climatological annual cycle as determined by data assimilation and will serve as the first guess/reference for the experiments performed here.

The main difference of the experiments performed in this paper to the FIN experiment in WSO concern the employed SSH data. While WSO use a mean annual cycle from the years 1993–95, we will perform two independent experiments, TOP95 and TOP96, using the measured annual cycles from 1995 and 1996 respectively. In both cases we will look for a cyclo-stationary solution thus taking the corresponding data as perpetual, e.g. we will employ a cyclic repetition of the annual cycle of the data while integrating the model for five years. The SSH data are obtained from the NASA/GSFC Ocean Pathfinder Project.

As in WSO we will constrain the annual mean SSH and the monthly anomalies seperately, where the two respective annual means of the data are refered to the EGM96 geoid (Lemoine et al., 1997). The climatological data used are the same as in WSO. They comprise the climatological annual cycle of temperature and salinity from the World Ocean Atlas WOA94 (Levitus et al., 1994; Levitus and Boyer, 1994), estimates of the annual mean transports of heat, mass and freshwater (Macdonald, 1995; Sloyan, 1997; Wijffels et al., 1992) as well as constraints on the mean Atlantic overturning and the cyclo-stationarity of the solution. Likewise, the control parameters that will be optimized by the adjoint method are the same as in WSO: the initial model state (temperature, salinity, SSH) and the monthly forcing fields (air temperature, surface freshwater flux, windstress).

Because we treat the data as perpetual, changes in the initial state of the model will become most obvious in the annual mean. Changes in the respective annual cycles will be caused mainly by different annual cycles of the forcing. However from our results we cannot discern the respective optimal forcings significantly. Therefore we will concentrate on the interpretation of the differences in the model's optimal annual mean states in Section 3.

In contrast to WSO we will use SSH data from specific years, while the other data employed describe climatology. To obtain a model state representative for the respective years the impact of the climatological datasets has to be reduced. This is done by increasing the weights for altimetry by a factor of 10 as compared to WSO. This factor appeared to be a reasonable compromise to achieve a good fit to the TOPEX/Poseidon data while departing not too far from the given hydrography. A larger factor surely would further improve the SSH fit but at the expense of degenerating the models hydrographic state and consequently its circulation and transports.

3. Results

Table 1 shows that the TOPEX/Poseidon data are well reproduced in the experiments TOP95 and TOP96 respectively. Their root mean square (RMS) deviations from the data are much less than in the reference FIN, especially if FIN is compared to the corresponding SSH data from 1995 and 1996. This is true for the monthly anomalies as well as for the annual means. Consequently the difference of the 1995 and 1996 annual mean SSH is well reproduced also (Fig. 1, Table 2). The model is able to reproduce about 70% of the spatial variance of the difference although it slightly overestimates its amplitude. This is expressed by the slope of the regression from model to data that is only 0.93.

As compared to the reference FIN temperature and salinity depart further from the WOA94 climatology (Table 1). But this is intelligible because in TOP95 and TOP96 the relative weights for the corresponding datasets in the cost function are reduced, which is equivalent to employing larger error bars. Although the latter ex-

Table 1
RMS value of the differences between the model solutions and the corresponding data

Experiment name	Year	TOPEX/Poseidon		WOA94 (0–125 m)	
		Mean (cm)	Anomalies (cm)	Temperature (K)	Salinity (psu)
FIN	93–95	13.2	1.27		
	95	13.3	2.02	1.21	0.283
	96	13.1	2.11		
TOP95	95	4.64	0.38	1.98	0.347
TOP96	96	3.88	0.28	1.95	0.340

Details about the reference solution FIN are given in Wenzel et al. (2001).

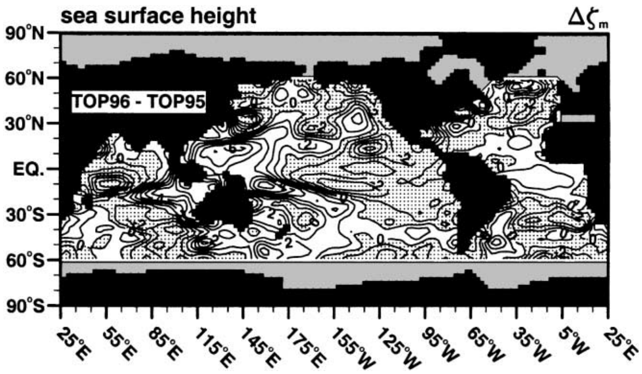

Fig. 1. Annual mean SSH difference, $\Delta\zeta_m$ between model solutions TOP95 and TOP96. Only the area with TOPEX/Poseidon data is shown. Stippled areas exhibit negative values. Contour interval: 1 cm.

periments have similar RMS deviations as compared to WOA94, their temperatures and salinities show up quite different. Most of these differences appear in the uppermost 250–500 m (Fig. 2). Only in regions with deep convection we also find changes in the deeper layers down to the bottom.

In view of these differences in density (temperature and salinity) and in the SSH we find only marginal changes in the circulation of the single model solutions. Nor there are notable differences in the forcing fields, which might have been a candidate to explain the insignificant impact on the circulation. Therefore it has to be conducted that the changes in the pressure field due to changes in density and SSH respectively mutually compensate, i.e. we have to take into account the steric effect due to thermal and haline expansion. The changes in SSH due to thermal and haline expansion are computed without any simplification as:

$$\Delta\zeta_{mT} = \int_{-H}^{\zeta} \frac{1}{\alpha} \frac{\partial\alpha}{\partial T}\bigg|_{S,p} \Delta T \,\mathrm{d}z$$

and

$$\Delta\zeta_{mS} = \int_{-H}^{\zeta} \frac{1}{\alpha} \frac{\partial\alpha}{\partial S}\bigg|_{T,p} \Delta S \,\mathrm{d}z$$

Table 2
Linear regression between different annual mean SSH differences

$x \to y$	Offset	Slope	Correlation
$\Delta\zeta_m$[a] $\to \Delta\zeta_{T/P}$[b]	0.0314	0.9280	0.8397
$\Delta\zeta_{mT}$[c] $\to \Delta\zeta_m$	−0.9122	0.7648	0.8316
$\Delta\zeta_{mS}$[d] $\to \Delta\zeta_m$	−0.0584	−0.1435	−0.1090
$\Delta\zeta_{mS} \to \Delta\zeta_{mT}$	1.0738	−0.8339	−0.5957
$\Delta\zeta_{mS} \to \Delta\zeta_m - \Delta\zeta_{mT}$	−1.1322	0.6904	0.8290
$\Delta\zeta_{mT} + \Delta\zeta_{mS} \to \Delta\zeta_m$	−1.1640	1.0490	0.9062

All analysis is restricted to the region where TOPEX/Poseidon data ($\Delta\zeta_{T/P}$) are available.
[a] Difference between model solutions TOP95 and TOP96.
[b] Difference from 1995/96 TOPEX/Poseidon data.
[c] Difference caused by thermal expansion.
[d] Difference caused by haline expansion.

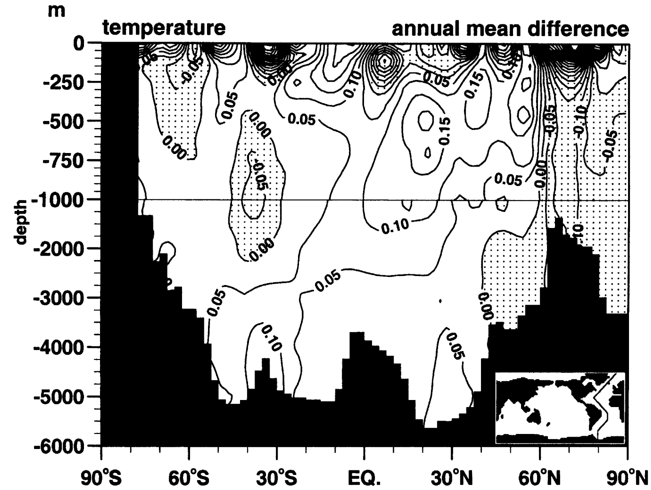

Fig. 2. Annual mean temperature difference from the model solutions, TOP96–TOP95, on the Atlantic section shown in the lower right inlet. Stippled areas exhibit negative values. Contour interval: 0.05 K.

respectively, where $\alpha = 1/\varrho$ is the specific volume of sea water, T—temperature, S—salinity and p—pressure. The expansion coefficients $e = (1/\alpha)(\partial\alpha/\partial T)$ and $h = (1/\alpha)(\partial\alpha/\partial S)$ respectively are derived from the UNESCO formula for density $\varrho = \varrho(S, T, p)$ (UNESCO (1981)) as it is used in the LSG model.

To demonstrate the concerted acting of the thermal and haline expansion, $\Delta\zeta_{mT}$ and $\Delta\zeta_{mS}$ respectively, these contributions to the annual mean SSH difference are shown along the zonal line 11°N (Fig. 3). First of all Fig. 3 confirms that the differences $\Delta\zeta_{T/P}$ as given by the TOPEX/Poseidon data are well reproduced by the models difference $\Delta\zeta_m$, TOP96–TOP95. Additionally we find different situations for the varying role of $\Delta\zeta_{mT}$ and $\Delta\zeta_{mS}$. While most of $\Delta\zeta_m$ can already be explained by $\Delta\zeta_{mT}$ in the western part of the Indian Ocean and in the Pacific, $\Delta\zeta_{mT}$ and $\Delta\zeta_{mS}$ have the same magnitude but opposit sign in the eastern part of the Indian Ocean and in the Atlantic. Here they nearly cancel.

In total $\Delta\zeta_{mT}$ (Fig. 4a) is capable of reproducing about 69% of the spatial variance in $\Delta\zeta_m$ (Table 2), i.e. the correlation amounts to 0.83, but the amplitude of the thermal expansion appears too big as indicated by the slope of the regression which is only 0.76. This overshooting of the thermal expansion is compensated by the halosteric effect, $\Delta\zeta_{mS}$ (Fig. 4b), whose sign usually is opposite to the thermal at least in most parts of the world ocean and whose horizontal structure is similar to that of $\Delta\zeta_{mT}$, thus leading to a negative correlation (Table 2). Both fields show values ranging from −5 to +8 cm. Maximum values in $\Delta\zeta_{mT}$ we find in the Atlantic and in the western tropical Pacific as well as in the eastern part of the Indian Ocean (Fig. 4a). For $\Delta\zeta_{mS}$ we find the largest positive value at the boundaries and in the region south of Africa. The largest negative halosteric changes are located in the southern Indian Ocean

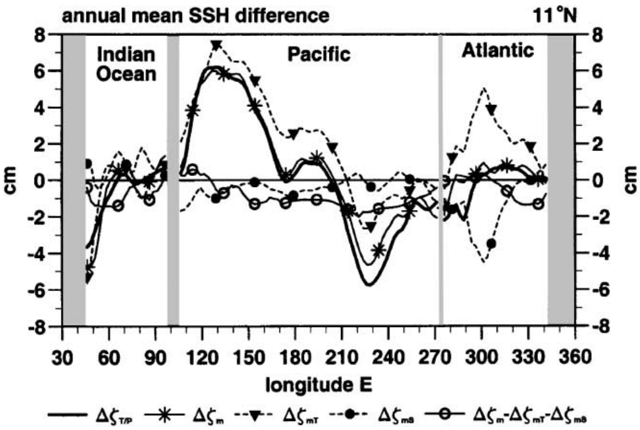

Fig. 3. Annual mean SSH difference, $\Delta\zeta_m$ (solid line with asterisk), from the model solutions, TOP96–TOP95, along the zonal section 11°N as compared to TOPEX/Poseidon, $\Delta\zeta_{T/P}$ (thick solid line). $\Delta\zeta_m$ is split into the parts caused by thermal and by haline expansion, $\Delta\zeta_{mT}$ (dashed with triangles) and $\Delta\zeta_{mS}$ (dashed with dots) respectively, as well as the residual, $\Delta\zeta_m - \Delta\zeta_{mT} - \Delta\zeta_{mS}$ (solid with circles) which is due to changes in the circulation.

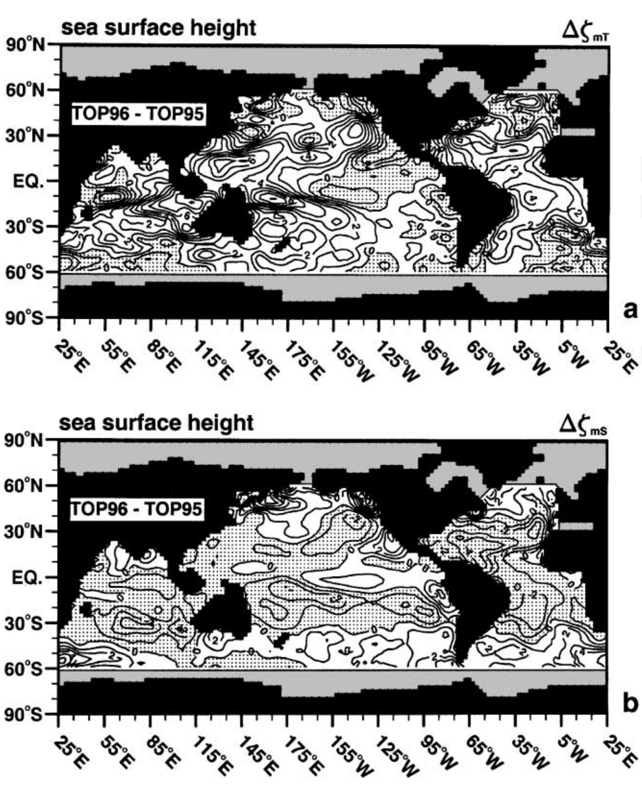

Fig. 4. Annual mean SSH difference between model solutions TOP95 and TOP96 caused (a) by the thermosteric effect, $\Delta\zeta_{mT}$, and (b) by the halosteric effect, $\Delta\zeta_{mS}$. Stippled areas exhibit negative values. Contour interval: 1 cm. As in Fig. 1 only the area with TOPEX/Poseidon data is shown.

and especially in the tropical North Atlantic where it nearly compensates the thermosteric.

Although $\Delta\zeta_{mS}$ has only low correlation to the total SSH differences $\Delta\zeta_m$ (−0.11) it reflects the difference

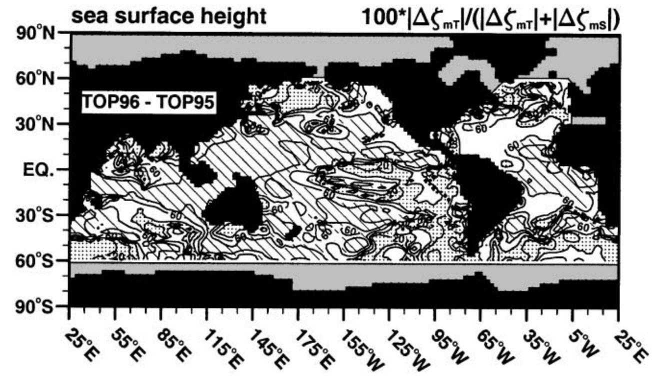

Fig. 5. Relative magnitude of the thermal and the haline expansion in percent. High values (hatched, above 60) indicate that the main contribution to the SSH changes stem from thermal expansion, while low values (stippled, below 40) indicate the dominance of the halosteric effect. In areas with no special signature thermosteric and halosteric effect nearly compensate each other because of their opposite sign. Contour interval: 20. As in Fig. 1 only the area with TOPEX/Poseidon data is shown.

$\Delta\zeta_m - \Delta\zeta_{mT}$ well. Consequently the combined thermohaline expansion explains the SSH differences best. The correlation is improved to be 0.91 now, i.e. $\Delta\zeta_{mT} + \Delta\zeta_{mS}$ is responsible for about 83% of the spatial variance in $\Delta\zeta_m$. Furthermore the slope of the regression is improved from 0.76 considering thermal expansion only to 1.05 including the halosteric effect. We only partly agree with Gill and Niiler (1973) that the latter plays a minor role. Concerning the magnitude this is true in many parts of the global ocean. But there are also large regions, especially the south-east Pacific and much of the Atlantic, where $\Delta\zeta_{mS}$ exceeds the thermosteric effect or at least has a comparable magnitude (Fig. 5). Furthermore the thermosteric and the halosteric effect are anticorrelated (Table 2), thus compensating each other. Therefore the halosteric effect should not be neglected anywhere! Similar results are obtained e.g. by Maes (1998), who investigates the results of different model configurations, or by Levitus and Antonov (2002), who compute the influence of temperature and salinity changes on the dynamic topography from measurements. Furthermore Sato et al. (2000) demonstrated the improvents achieved in estimating the heat storage changes from TOPEX/Poseidon when additionally considering salinity changes. Finally, only a minor SSH residual, $\Delta\zeta_m - \Delta\zeta_{mT} - \Delta\zeta_{mS}$, remains that contributes to changes of the pressure field (Fig. 6) and because of its weak gradients it has only little influence on the circulation.

4. Summary and conclusions

This paper demonstrates the capability of the LSG model to reproduce the differences in the annual mean SSH for 1995 and 1996 as seen by the TOPEX/Poseidon

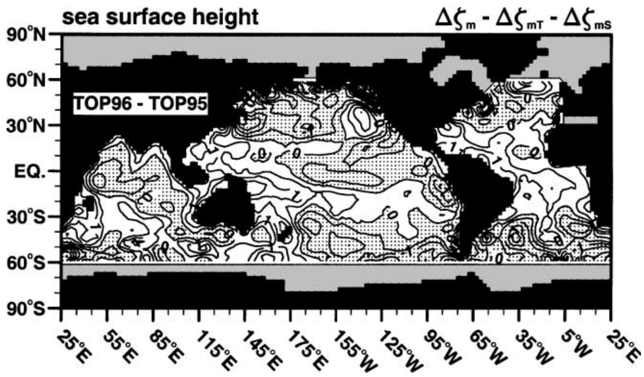

Fig. 6. The residual part of the models SSH difference, $\Delta\zeta_m - \Delta\zeta_{mT} - \Delta\zeta_{mS}$, that contributes to pressure field changes at depth. The area mean value as given by the offset in Table 2 (last row) has been removed because it has no bearing on the circulation. Stippled areas exhibit negative values. Contour interval: 0.5 cm. As in Fig. 1 only the area with TOPEX/Poseidon data is shown.

altimeter. It appears that the resulting SSH differences have only little influence on the circulation. A detailed inspection of the results showed that the optimization method prefers to change the initial thermo-haline structure, i.e. the density field of the model, instead of changing the forcing fields to achieve a good cyclo-stationary solution. Most of these changes in density appear in the uppermost 250–500 m of the water column. Only in regions with deep convection we also find changes in the deeper layers down to the bottom. They compensate the SSH differences, thus there are only minor differences in the pressure field which is the main defining quantity for the velocities. Due to the steric effect the changed thermo-haline structure is responsible for about 82% of the modelled SSH differences. 69% of the total can already be explained by thermal expansion which is the dominant effect in most of the global ocean. The haline expansion usually is weaker than the thermal one, but because they are anti-correlated they partly compensate. Therefore one should not neglect the halosteric effect when interpreting SSH differences.

Acknowledgements

This work was supported by the HGF Strategiefonds Projekt 2000/13 SEAL. The authors wish to thank C.K. Shum and an anomymous reviewer for their comments that led to an improvement of the manuscript.

References

Gill, A.E., Niiler, P.P., 1973. The theory of the seasonal variability in the ocean. Deep Sea Research 20, 141–177.

LeDimet, F.-X., Talagrand, O., 1986. Variational algorithms for analysis and assimilation of metereological observations: theoretical aspects. Tellus 38A, 97–110.

Lemoine, F.G., Smith, D.E., Kunz, L., Smith, R., Pavlis, E.C., Pavlis, N.K., Klosko, S.M., Chinn, D.S., Torrence, M.H., Williamson, R.G., Cox, C.M., Rachlin, K.E., Wang, Y.M., Kenyon, S.C., Salman, R., Trimmer, R., Rapp, R.H., Nerem, R.S., 1997. The development of the NASA GSFC and NIMA joint geopotential model. In: Segawa, J., Fujimoto, H., Okubo, S. (Eds.), Gravity Geoid and Marine Geodesy, Vol. 117. International Association of Geodesy Symposia, pp. 461–469.

Levitus, S., Antonov, J., 2002. Steric sea level variations during 1955–95. Physics and Chemistry of the Earth, this issue.

Levitus, S., Burgett, R., Boyer, T., 1994. World Ocean Atlas 1994, vol. 3. Salinity, NOAA Atlas NESDIS 3. US Department of Commerce, Washington, DC.

Levitus, S., Boyer, T., 1994. World Ocean Atlas 1994, vol. 4. Temperature, NOAA Atlas NESDIS 4, US Department of Commerce, Washington, DC.

Macdonald, A.M., 1995. Oceanic fluxes of mass, heat and freshwater: a global estimate and perspective. PhD thesis, Department of Earth, Atmospheric and Planetary Sciences, MIT, Cambridge 02139, p. 326.

Maes, C., 1998. Estimating the influence of salinity on sea level anomaly in the ocean. Geophysical Research Letters 25, 3551–3554.

Maier-Reimer, E., Mikolajewicz, U., 1991. The Hamburg Large Scale Geostrophic Ocean General Circulation Model (Cycle 1). Technical Report No. 2, Deutsches Klimarechenzentrum, Hamburg, p. 34.

Maier-Reimer, E., Mikolajewicz, U., Hasselmann, K., 1993. Mean circulation of the Hamburg LSG OGCM and its sensitivity to the thermohaline surface forcing. Journal of Physical Oceanography 23, 731–757.

Marchuk, G.I., 1975. Formulation of the theory of pertubations for complicated models–Part I: the estimation of climate change. Geofisica Internacional 15, 103–156.

Sato, O.T., Polito, P.S., Liu, W.T., 2000. Importance of salinity measurements in the heat storage estimation from TOPEX/Poseidon. Geophysical Research Letters 27, 549–551.

Sloyan, B., 1997. The circulation of the Southern Ocean and the adjacent ocean basins determined by inverse methods. PhD thesis, Institute of Antarctic and Southern Ocean Studies, University of Tasmania, p. 479.

Stammer, D., 1997. Steric and wind-induced changes in TOPEX/Poseidon large-scale sea surface topography observations. Journal of Geophysical Research 102, 20987–21009.

Thacker, W.C., 1988. Three lectures on fitting numerical models to observations, GKSS 87/E/65, GKSS Forschungszentrum, Geesthacht, p. 87.

UNESCO, 10th Report of the joint panel on oceanographic tables and standards, UNESCO Technical Papers in Marine Science, 36, UNESCO, Paris, 1981.

Vivier, F., Kelly, K.A., Thompson, L., 1999. Contributions of wind forcing, waves, and surface heating to sea surface height observations in the Pacific Ocean. Journal of Geophysical Research 104, 20767–20788.

Wenzel, M., Schröter, J., Olbers, D., 2001. The annual cycle of the global ocean circulation as determined by 4D VAR data assimilation. Progress in Oceanography 48, 73–119.

Wijffels, S.E., Schmitt, R.W., Bryden, H.L., Stigebrandt, A., 1992. Transport of freshwater by the ocean. Journal of Physical Oceanography 22, 155–162.